



---

Applied Computational  
Electromagnetics Society

---



Newsletter  
Volume 22 – No. 3  
ISSN 1056-9170



November 2007





**APPLIED COMPUTATIONAL ELECTROMAGNETICS SOCIETY  
(ACES)**

**NEWSLETTER**

Vol. 22 No. 3

November 2007

**TABLE OF CONTENTS**

EDITORS COMMENT.....	2
CALL FOR PAPERS – ACES 2008 .....	3
PERSPECTIVES IN CEM	
“Quantifying Error and Uncertainty in CEM” Robert S. Edwards, Andy C. Marvin, Stuart J. Porter .....	5
TECHNICAL FEATURE ARTICLE	
“Comparisons of CEM Predictions to IR Images of EM Fields for Complex Systems” John Norgard, Randall Musselman, Irina P. Kasperovich, Andrew L. Drozd .....	9
TUTORIAL	
“Prediction and Mitigating Techniques of the PCB Rectangular Power/Ground Planes’ Resonance Modes” Sungtek Kahng.....	15
ANNOUNCEMENTS:	
COMMITTEES AND RESPONSIBILITIES .....	24
ADVERTISING RATES .....	28
DEADLINE for Submission of Articles.....	28
LAST WORD ... ..	28

## Editor's comment

It is nice to be part of the ACES Newsletter and I would like to thank Bruce for being such a hard act to follow.

When Bruce floated the idea past me of taking the reins, I looked a little deeper into the history of ACES – that is, I clicked on the History tab on the ACES website and read the very informative work of Robert Bevensee. The first part of this put the purpose of the Newsletter into perspective:

*The ACES organization began as a four-day workshop followed by several newsletters and grew into an international corporation in only five years for several crucial reasons. It filled a need among electrical engineers working in the field of electromagnetic phenomena computation and a relatively small but intensely dedicated coterie of professionals and their organizations supported the ACES' activities.*

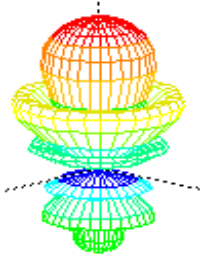
The Newsletter is about the communication between Acesians and I hope that I can successfully follow this ostensibly simple objective and help share opinion, news and good practice through the community. To this end, please consider the Newsletter, your Newsletter, as a vehicle to communicate with the rest of the Acesian community in passing on information or, in fact, seeking it.

I look forward to hearing from you.

Best wishes

Alistair

[apd@dmu.ac.uk](mailto:apd@dmu.ac.uk)



# ACES

## Applied Computational Electromagnetics Society



ACES Web Site: <http://aces.ee.olemiss.edu>

### CALL FOR PAPERS

**The 24<sup>th</sup> International Review of Progress in Applied Computational Electromagnetics (ACES 2008)**  
**March 30 – April 4, 2008**  
**Hilton Fallsview, Niagara Falls, Canada**

The purpose of the international annual ACES Symposium is to bring developers, analysts, and users together to share information and experience about the practical application of electromagnetic analysis using computational methods. The symposium offers technical presentations, software demonstrations, vendor booths, short courses, and hands-on workshops. The ACES Symposium is a highly influential international forum promoting awareness of recent technical contributions to the advancement of computational electromagnetics.

Papers address general issues in applied computational electromagnetics or may focus on specific applications, techniques, codes, or computational issues of potential interest to the Applied Computational Electromagnetics Society membership. The following is a list of suggested topics, although contributions in other areas of computational electromagnetics are encouraged and will be considered.

#### Suggested Topics:

Integral Equation Methods	Wideband and Multiband Antennas
Differential Equation Methods	Dielectric Resonator Antennas
Fast and Efficient Methods	Phased Array Antennas
Hybrid and Multi-Physics Modeling	Smart Antenna and Arrays
EM Modeling of Complex Mediums	EBG and Artificial Materials
Inverse Scattering and Imaging Techniques	Frequency Selective Surfaces
Optimization Techniques for EM-based Design	MEMS-NEMS and MMIC
Asymptotic and High Frequency Techniques	EMC/EMI
Low Frequency Electromagnetics	Propagation
Computational Bio-Electromagnetics	Remote Sensing
Printed and Conformal Antennas	RF and Microwave Devices

All authors of accepted papers will have the option to submit an extended version of their paper or papers for review and publication in a special issue of the ACES Journal.

#### SYMPOSIUM STRUCTURE

The international annual ACES Symposium traditionally includes: (1) oral sessions, regular and invited, (2) poster sessions, (3) a student paper competition, (4) short courses, (5) software demonstration, (6) an awards banquet, (7) vendor exhibits, and (8) social events. The ACES Symposium also includes plenary and panel sessions, where invited speakers deliver original essay-like reviews of hot topics of interest to the computational electromagnetics community.

## **PAPER FORMATTING REQUIREMENTS**

The recommended paper length, including text, figures, tables and references, is four (4) pages, with six (6) pages as a maximum. Submitted papers should be formatted for printing on 8.5x11-inch U.S. standard paper, with 1 inch top, bottom, and side margins. On the first page, the title should be 1-1/2 inches from top with authors, affiliations, and e-mail addresses beneath the title. Use single line spacing, with 11 or 12-point font size. The entire text should be fully justified (flush left and flush right). No typed page numbers. A sample paper can be found in the conference section on ACES web site at: <http://aces.ee.olemiss.edu>. Each paper should be submitted in camera-ready format with good resolution and clearly readable.

## **PAPER SUBMISSION PROCEDURE**

**No email, fax or hard-copy paper submission will be accepted.** Photo-ready finished papers are required, in Adobe Acrobat format (\*.PDF) and must be submitted through ACES web site using the “Upload” button in the left menu, followed by the selection of the “Conference” option, and then following the on-line submission instructions. Successful submission will be acknowledged automatically by email after completing all uploading procedure as specified on ACES web site.

## **SUBMISSION DEADLINE AND REGISTRATION REQUIREMENT**

Submission deadline is **November 16, 2007**. A signed ACES copyright-transfer form must be mailed to the conference technical chair immediately following the submission as instructed in the acknowledgment of submission email message. Papers without an executed copyright form will not be considered for review and possible presentation at the conference. Upon the completion of the review process by the technical program committee, the acceptance notification along with the pre-registration information will be emailed to the corresponding author on or about **January 15, 2008**. Each presenting author is required to complete the paid pre-registration and the execution of any required paper corrections by the firm deadline of **January 31, 2008** for final acceptance for presentation and inclusion of accepted paper in the symposium proceedings.

## **BEST STUDENT PAPERS CONTEST**

The best three (3) student papers presented at the 24<sup>th</sup> Annual Review will be announced at the symposium banquet. Members of the ACES Board of Directors will judge student papers submitted for this competition. The first, second, and third winners will be awarded cash prizes of **\$300, \$200, and \$100**, respectively.

For questions please contact the conference chair **Dr. Natalia Nikolova** (905) 525 3189 ext. 27141, [talia@mcmaster.ca](mailto:talia@mcmaster.ca) or visit ACES on-line at: <http://aces.ee.olemiss.edu>

<b>General Chairs</b>	<b>Technical Program Chair</b>	<b>Short Course Chair</b>	<b>Exhibits Chair</b>	<b>Publicity Chair</b>
<i>Natalia Nikolova and Mohamed Bakr</i>	<i>Atef Elsherbeni</i>	<i>Amir Zaghloul</i>	<i>Andrew L. Drozd</i>	<i>C. J. Reddy</i>
McMaster University	The University of Mississippi	Virginia Tech	ANDRO Consulting	EM Software & Systems

## Quantifying Errors and Uncertainty in CEM

Robert S. Edwards, Prof. Andy C. Marvin and Dr. Stuart J. Porter

Contact Robert Edwards [rse101@ohm.york.ac.uk](mailto:rse101@ohm.york.ac.uk)

At the University of York, research is being conducted to determine possible methods for quantifying the errors and uncertainties that exist in Computational Electromagnetics (CEM) simulations. Standards already exist that require an estimate of the uncertainty in measurements obtained from laboratory Electromagnetic Compatibility (EMC) measurements [1]. Currently no requirement exists for the measurements obtained by CEM simulations. Such error and uncertainty analyses would allow different models to be compared for accuracy. The analyses would help determine quantitatively whether a computationally cheaper, less accurate model, is accurate enough for purpose. Knowledge of the error and uncertainty in the output of a simulation would also provide a quantitative level of confidence in the results.

The ‘Guide to the Expression of Uncertainty in Measurement’ [2] provides a framework for quantifying uncertainties in measurements. It is currently the internationally accepted master document for quantifying uncertainties [3]. This guide describes the error in a measured value as the difference between the measured value and the true value of the measurand [2]. It describes the uncertainty in the measured value as the quantification of the doubt about the measured value [2]. These descriptions of error and uncertainty are generally applicable to all types of measurement. It is possible to make more explicit definitions when considering the errors and uncertainties in computer modelling.

Currently there has been more work on error and uncertainty analyses in Computational Fluid Dynamics (CFD) [4] - [7] than in CEM, and so this discipline is chosen to provide a formal definition of the errors and uncertainties in computer models. The following definitions come from the American Institute of Aeronautics and Astronautics (AIAA) report on the verification and validation of CFD simulations [5].

*Error: A recognizable deficiency in any phase or activity of modelling and simulation that is not due to lack of knowledge.*

Errors are introduced into our models via the approximations and assumptions that are made in forming the model. Since these approximations and assumptions are generally known, the errors they produce can be analysed [4]. One type of error in conventional FDTD is the staircasing error that arises from modelling a curved surface on a rectangular grid. The modelled surface is *known* to be inaccurate and this inaccuracy will manifest itself as an error in the final measured value.

*Uncertainty: A potential deficiency in any phase or activity of the modelling process that is due to lack of knowledge.*

Uncertainties can be further categorized into two groups. The first is the uncertainty in how well the mathematical model represents the true behaviour of the real physical system [7]. This uncertainty is very difficult to determine [7]. Electromagnetism is mathematically represented by Maxwell's Equations, which have been verified by many people over many years. Thus it may be assumed that the model uncertainty can be ignored in CEM. The second type of uncertainty is the uncertainty that arises due to a lack of precise input parameter data [7]. If there are uncertainties in the input parameter data, then there will be uncertainties in the output. This type of uncertainty is often known as parameter uncertainty [7].

### Determining Errors

In order to determine the errors that exist in a model, an error taxonomy must first be formed. This taxonomy is a list of all the possible sources of error that may exist in the simulation. The errors in this list may be quantified by considering the approximations and/or assumptions that have caused them. This is not a trivial task and may be computationally expensive.

In FDTD, one known source of error is the discretisation of space and time. This can be analysed by comparing the results of one simulation with the results of the same simulation, performed on a finer mesh. As the mesh size decreases so does the error in the simulation. Thus an estimate of the error in the less accurate simulation can be formed by comparing the results of this simulation with that of the more accurate simulation.

### Determining Parameter Uncertainties

Uncertainty analyses are either possibilistic or probabilistic. The work at York concentrates on the probabilistic methods. Probabilistic methods use the known Probability Density Functions (PDFs) of the input parameters to estimate the mean output value, and the combined uncertainty in this value. Three methods that are currently being investigated are the: Method of Moments (MOM), Monte Carlo Method (MCM) and Polynomial Chaos Method (PCM) [8]-[10].

The MOM is similar to the method outlined in UKAS [1] for the determination of uncertainty in practical EMC measurements. It is the method outlined in the 'Guide to the Expression of Uncertainty in Measurement' [2], for the propagation of uncertainties through a model. This method first calculates the uncertainty in the output due to each of the individual uncertain parameters; these individual output uncertainties are then combined to form the combined output uncertainty. It seems that this method is computationally the cheapest, but not the most accurate.

The MCM involves taking multiple samples of the input parameters from their respective PDFs, performing multiple simulations using these samples, and then combining the multiple outputs to form an output PDF. The combined output uncertainty is taken to be the standard deviation of this PDF. This method is much more expensive computationally, but provides the most rigorous analysis of the uncertainty.



In the PCM, the solution is assumed to be the expansion of certain orthogonal basis polynomials, which represent the individual input uncertainties. These polynomials are propagated through the model and the combined uncertainty is found from the outputs. This method has been found to predict uncertainties that agree with those predicted by the more rigorous MCM. The PCM is slower than the MOM but much faster than the MCM. The memory requirements for the PCM are much bigger than both the other methods described here. This may limit its applicability to more complex simulations. The PCM has already been applied to one area of CEM [11]. Through this work it was shown that the PCM can accurately estimate uncertainties much more quickly than the MCM for a number of applications.

All of the above uncertainty analyses require extra computational expense. The determination of uncertainty in laboratory measurements also requires extra work. At the University of York an uncertainty analysis method is currently being sought which will require minimal computational expense. This method will use a prior knowledge based expert system, informed by economic use of the techniques described above, applied to the current problem.

### Conclusion

Error and uncertainty analyses would help us quantitatively compare the accuracy of different models in CEM. The analyses would also provide us with a quantitative level of confidence in the results obtained from these models. The formulation of such analyses is not a trivial task. Errors may be determined by using the results of more accurate simulations. Uncertainties can be determined in many different ways: some methods are more accurate, but other methods are computationally cheaper. All the uncertainty analyses described here require significant extra computational expense; the laboratory derivation of experimental uncertainty also requires a significant expense. Work is currently being carried out to determine whether it is possible to estimate the combined uncertainty in a simulation with only a small amount of extra computational expense. This work is based on using the techniques described above to update a prior knowledge based expert system.

### References

- [1] The Expression of Uncertainty in EMC Testing. UKAS publication LAB 34, Edition 1, 2002.
- [2] Guide to the Expression of Uncertainty in Measurement, ISO, Geneva, Switzerland, 1993 (ISBN 92-67-10188-9).
- [3] M. G. Cox and B. R. L. Siebert. The use of a Monte Carlo method evaluating uncertainty and expanded uncertainty. *Metrologia*. 43:S178-S188, 2006.
- [4] R. W. Walters and L. Huyse. Uncertainty analysis for fluid dynamics with applications. ICASE Report no. 2002-1, NASA/CR-2002-211449, 2002.
- [5] AIAA, Guide for the verification and validation of computational fluid dynamics simulations, AIAA G-077-1998, 1998.

- [6] R. E. Moore. Interval Analysis. Prentice-Hall, 1966.
- [7] J. Faragher. Probabilistic methods for the quantification of uncertainty and error in computational fluid dynamics simulations. DSTO Air Vehicles Division, DSTO-TR-1633, 2004.
- [8] N. Wiener. The homogeneous chaos. American Journal of Mathematics, 60:897-936, 1938.
- [9] R.G. Ghanem and P. Spanos. Stochastic Finite Elements: a Spectral Approach. Springer, 1991.
- [10] D.B. Xiu and G.E. Karniadakis. The Wiener-Askey polynomial chaos for stochastic differential equations. SIAM Journal on Scientific Computing. 24(2):619-644, 2002.
- [11] C. Chauviere, J.S. Hesthaven and L. Lurati. Computational modeling of uncertainty in time-domain electromagnetics. SIAM Journal on Scientific Computing. 28(2):751-775, 2006.

# COMPARISONS OF CEM PREDICTIONS TO IR IMAGES OF EM FIELDS FOR COMPLEX SYSTEMS

John Norgard  
US AFRL/RRS(SNRT)  
Rome, NY, USA

Randall Musselman  
US Air Force Academy, DFEC  
Colorado Springs, CO, USA

Irina P. Kasperovich and Andrew L. Drozd  
ANDRO Computational Solutions, LLC  
Beeches Technical Campus  
7902 Turin Road, Ste. 2-1  
Rome, NY, USA

## ABSTRACT

An infrared (IR) measurement technique, based on thermal principles, is presented to independently validate and verify (V&V) numerical codes used for computational electromagnetic (CEM) field predictions. This technique is applied to scattering and to complex systems such as antennas on aircraft. The IR technique produces a thermal image of the EM field over any two-dimensional area, usually a plane, proportional to the intensity of the incident EM field being measured. This IR image can be compared to the predicted image of the field calculated with a numerical CEM code over the same plane that was used in the measurements to confirm the field patterns. Precise thermal measurements on metallic scale models of canonical aircraft shapes are made in a controlled anechoic chamber environment. The scattered fields from the model are measured for different test setups. The temperature distribution is converted to field intensity and plotted as a false color image of the field and compared to similar plots from a selected CEM code. The field can also be visualized with this IR method. This is the first step in a progressive approach to compare results of more sophisticated geometries using a suite of CEM codes to confirm the results of the IR measurements and to develop confidence in the complementary measurement and simulation methods.

Keywords: Electromagnetic Scattering, Infrared Measurements, Computational Electromagnetics, Computer Model Verification and Validation, Standards

## 1.0 Introduction

This paper describes an effort to compare two different methods of predicting the scattered fields for a complex arrangement of canonical objects that resemble an aircraft system. In particular, this effort was to first measure the scattered fields for a selected test article using a horn antenna test setup in conjunction with a novel IR measurement technique. Results were then compared to computer simulations of the same. The test article in this case is a highly simplified, canonical based geometry comprised of perfectly electrically conducting (PEC) plates, a fully-enclosed right circular cylinder and a cone. The physical measurements and computer simulations which are described below focused on irradiating the test article at a few select frequencies in the C-Band with a plane wave at a given polarization and a fixed nose-on position.

It was decided that in order to gain a better understanding of the electromagnetic (EM) phenomenology associated with the geometric scattering, a simplified canonical aircraft representation and limited test conditions would be considered as an initial step. This would provide a baseline understanding of the phenomenology. In the future, the plan is to extend this study using IR and computer simulation techniques to compare the predictions of electromagnetic scattering for more sophisticated systems representing real aircraft at multiple frequencies, different aspect angles, meta materials, etc.

In this paper, an IR measurement technique, based on thermal principles, was used to independently V&V a selected first-principles CEM code, which hybridizes the moment method (MoM) and uniform theory of diffraction (UTD) high-frequency ray tracing techniques. This code was used to predict the far-field scattering from the canonical aircraft

model. The scattered fields were then measured using the IR imaging method. The predicted fields were compared to the measured fields to V&V the code. This is the first in a series of tests to check the numerical codes. Later, the simple canonical model will be replaced by a high-fidelity model of a conventional aircraft, then, later yet, by a stealthy aircraft. The predicted and measured fields scattered by the conventional and stealth aircrafts will also be compared in the future.

Generally, in this process, precise thermal measurements on metallic scale models of canonical aircraft shapes are made in a controlled anechoic chamber environment with a radiating horn antenna to make scattered field measurements around the model. The temperature distribution is converted to field intensity, plotted as a false color image of the field, and compared to similar plots from various CEM codes. The field can also be visualized with this IR method. A selected CEM code is run to confirm the results of the IR measurements to develop confidence in the measurement and simulation methods.

## **2.0 IR Technique**

The IR technique produced thermal images of the EM fields over several planar two-dimensional areas, which were proportional to the intensity of the incident field [1, 2]. The images are presented as 2D contour plots or as 3D relief maps of the relative or absolute intensities of the EM fields being measured. Recall that this IR image is compared to the predicted image of the field calculated with the numerical CEM code over the same plane that was used in the measurements to confirm the field levels. In these comparisons, emphasis is placed on the qualitative similarities and differences (i.e., pattern comparisons), rather than performing a quantitative evaluation of field intensities. This is due to the fact that the false color scales are different between the IR/thermal method and the CEM tool used in the simulations. A technique is being examined to relate the two color bars and scales in order to better accommodate quantitative comparisons.

## **3.0 IR Setup**

The IR measurements were made by placing a thin, lossy (but, low loss) minimally perturbing detector screen in the plane over which the field is to be measured. As the field passes through the screen, some of the EM energy is absorbed by the lossy material of the screen (due to polarization, magnetization, and conduction losses). The absorbed energy causes the temperature of the screen to rise (Joule heating) over the background ambient temperature of the screen. An IR camera is used to measure the temperature distribution created across the screen. The temperature rise, on a pixel-by-pixel basis, is proportional to the local intensity of the EM field incident on the screen. This is a highly non-linear relationship due to the  $T^4$  temperature relationships for black-body radiation. The temperature rise over the background temperature for different screen materials as a function of the intensity of the field incident on the screen has been previously measured at NIST/Boulder to produce a calibration table of the incident field intensity vs. the color temperature of the screen material. Carbon loaded polyimide films are used for these tests that measure the electric field intensity of the EM field incident on the screen. This color table for each screen material (with different carbon loadings) is used to measure the absolute field intensity of the incident field based on the measured color temperature of the screen. The screen that will produce a significant temperature rise over the ambient temperature with the smallest amount of carbon loading, which will cause the smallest perturbation of the field being measured, is selected to measure the incident field.

## **4.0 IR Measurements**

Precise thermal measurements were made in a controlled anechoic chamber environment on a small canonical 1/32 scale model of a selected aircraft. The model consists of a right-cylindrical tube for the fuselage with a conical end cap on the front side and a flat end cap on the back side, as shown in Fig. 1. The wings were constructed from thin, flat, rectangular pieces of metal and were inserted through slots in the fuselage. The horizontal stabilizers were made similar to the wings, but shorter. The vertical stabilizer was triangular shaped and also inserted into a slot in the fuselage.

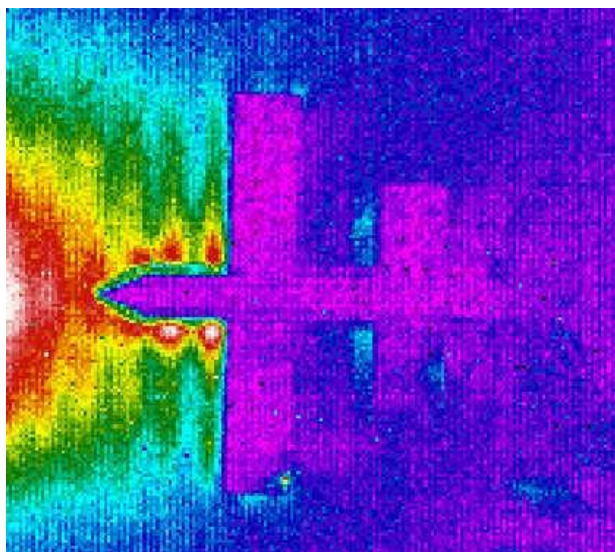
The thin detector screen material was taped onto a flat sheet of Styrofoam. The screen was used to measure the field in the plane of the wings and horizontal stabilizers of the aircraft. An outline of the 1/32 scale model aircraft was cut into the Styrofoam backed screen material and the model was embedded into screen and taped into position. The screen was just under the wings. The screen with the embedded model was placed inside the anechoic chamber on Styrofoam blocks and irradiated at several selected and representative frequencies, viz. from 4 to 8 GHz. The angle-of-incidence was nose-on. The polarization was in the (x-z) plane of the wings. Other angles-of-incidence and polarizations were also tested.

## 5.0 IR Images

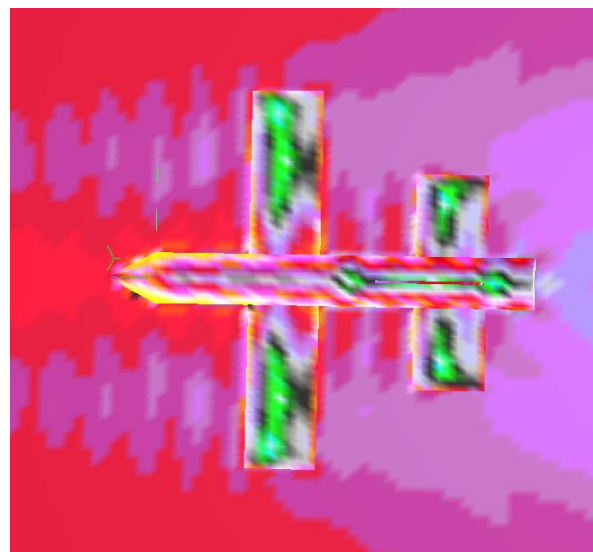
The scattered field was measured around the model. Normally, the resulting temperature distribution is converted to field intensity using a color table. However, in this example, the relative magnitudes were plotted as a contour map, as shown in Fig. 2a at several C-Band frequencies. These images were compared to similar plots from the selected MoM/UTD numerical code that was run for the same case.



**Figure 1. Anechoic Chamber and Test Article Setup with Horn Antenna and IR Camera**



(a)



(b)

**Figure 2. (a) Contour Map Showing Measured Relative Field Magnitudes at 3GHz Using the IR Technique, and (b) Contour Map Showing Relative Co-Pole Field Magnitudes Using a Plane Wave CEM Simulation Technique**

## 6.0 Computer Model

The computer model that was used for the simulations mimicked the basic test setup and conditions that were used for the IR measurements. The geometrical model was identical in form to the canonical model discussed above. It was generated in accordance with the 1/32 scale model dimensions used in the IR measurements. The geometrical objects used to represent the simulation model were all assumed to be PEC.

In the initial runs, both a dipole and a horn source were modeled independently in separate runs. A horizontal electric field polarization was assumed i.e., E-field in the plane of the wings. For accuracy purposes, the horn antenna required a very detailed description of the source feed and the horn structure at the various frequencies of interest. For simplicity and for the purposes of computational efficiency, and since the initial runs were meant to only verify the generalized scattering patterns from a qualitative viewpoint, the simulations focused on using a far-field dipole as the source instead of the horn antenna model. This provided sufficient results which could be used to perform the first-order comparisons to the IR measurements. For example, the predicted scattering at 3 GHz using the plane wave simulation approach is shown in Fig. 2b. Generally, the sampling criterion used in the MoM modeling was  $0.1\lambda$  where  $\lambda$  is the wavelength at the sample frequency.

## 7.0 Results and Observations

The original focus of this study was on the frequency of 3 GHz where some interesting scattering phenomena were observed both in the measured and in the simulated models. The structure of the field was visualized with the IR method. For example, the spherical standing wave setup between the horn antenna and the portion of the canonical aircraft where say a phased array radar antenna in the nose may be located, can be easily seen in Fig. 2a (indeed, this is the sort of problem that could be examined in the real world as pertaining to the F-16 Fire Control Radar or other fighter aircraft systems). In addition, the surface wave excited on both sides of the airframe between the tip of the fuselage and the ends of the wings can also be easily identified in the figure (another practical concern). The shadow zone behind the aircraft is also quite evident.

The corresponding simulation results are shown in Fig. 2b, for the horizontal co-pole plane wave case. The same essential features of the scattered wave are present in both the predicted and the measured waves. Note the differences in the color schemes between the measured and the predicted fields, which make the comparisons more difficult to correlate and match. Also, the thermal image is saturated in the standing wave area, so that some of the spherical wave patterns are obscured. Recall that for the initial cases studied, emphasis was on performing a qualitative comparison in order to identify consistent trends or any anomalies with respect to the results of the IR and computer simulation techniques.

The results of Figs. 2a and 2b show good agreement for the standing waves and scattering peaks and nulls in the vicinity of the front cone-cylinder portion of the overall geometry. In the computed model it was also observed that structural resonance currents and resultant standing waves were formed along the cylindrical tube, but are not clearly seen in Fig. 2b due to the relatively high intensity predicted currents and scattered fields. Upon closer examination of the results of Fig. 2b, the standing wave peaks can be more easily observed by changing the perspective of the viewpoint of the computed model.

Other higher frequency cases were also measured and modeled. In these tests, the computer model was changed from a plane wave source to a spherical source. In addition, an attempt was made to better correlate the color scales between the measured and the simulated results.

Figs. 3a and 3b compare the results between the measurement and the simulation for nose-on radiation at 4 GHz. The polarization is in the plane of the wings. The incident wave is clearly seen as a spherical wave. Many of the previously noted features of the scattered field distribution can be noted in the figures. Similarly, Figs. 4a and 4b compare the results between the measurement and the simulation for nose-on radiation at 6 GHz.

Figs. 5a and 5b compare the results between the measurement and the simulation for tail-on radiation at 4 GHz. The polarization, as above, is in the plane of the wings. Again, the incident wave is clearly seen as a spherical wave and, as before, many of the previously noted features of the scattered field distribution can be noted in the figures. Similarly, Figs. 6a and 7b compare the results between the measurement and the simulation for tail-on radiation at 6 GHz.



## 8.0 Summary

The primary emphasis of this study was on applying an IR measurement technique to independently V&V numerical codes used for CEM field predictions. This was done for a simple canonical metallic scale model of typical aircraft in the Air Force inventory. The immediate goal was to determine if two diverse and independent methods of determining the scattered fields could provide similar results relying on a first-level qualitative comparison. The results obtained were found to be in generally good agreement between the IR and computer simulation techniques, and deemed to be acceptable for the purposes of this initial phase of the study. Further examination of the results of RF measurements of the model will take place in the future and the approach will be expanded to look at more sophisticated aircraft models (e.g., F-16, F-35, etc.). Future studies will also account for multiple frequencies, different aspect angles, and materials. It is also noteworthy to mention that the results of this study will be of much benefit to the IEEE EMC Society Standards Development Committee; in particular, it will benefit the IEEE P1597 Working Group chartered with the development of standards and recommended practices for validating CEM techniques for EMC applications.

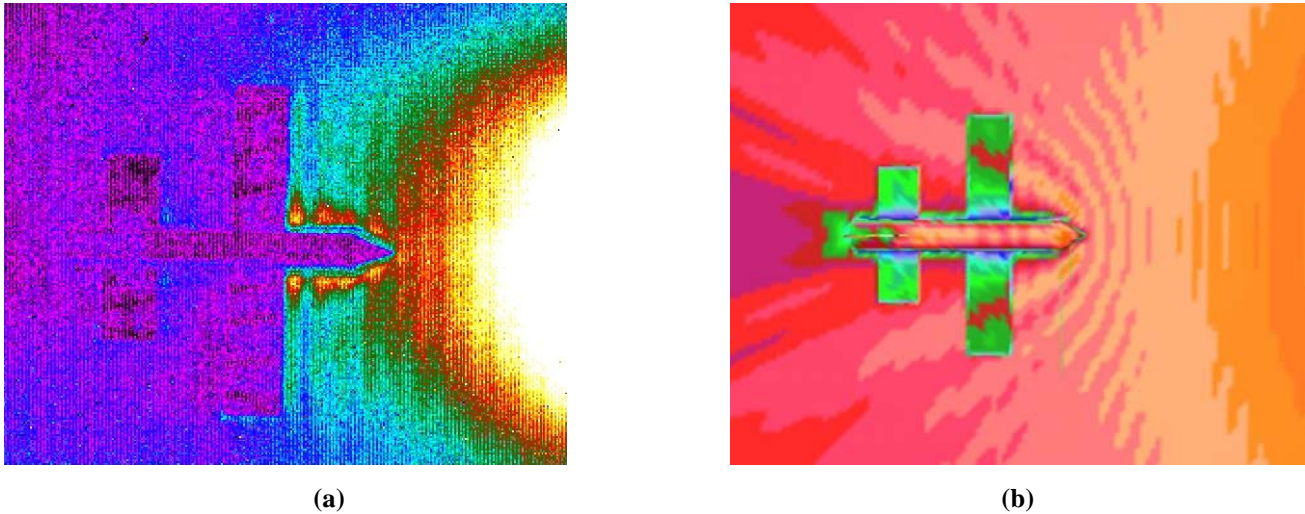


**Figure 3. Nose-On at 4GHz (Incident Spherical Wave)**  
**(a) Contour Map Showing Measured Relative Field Magnitudes Using the IR Technique, and**  
**(b) Contour Map Showing Relative Co-Pole Field Magnitudes Using the CEM Simulation Technique**

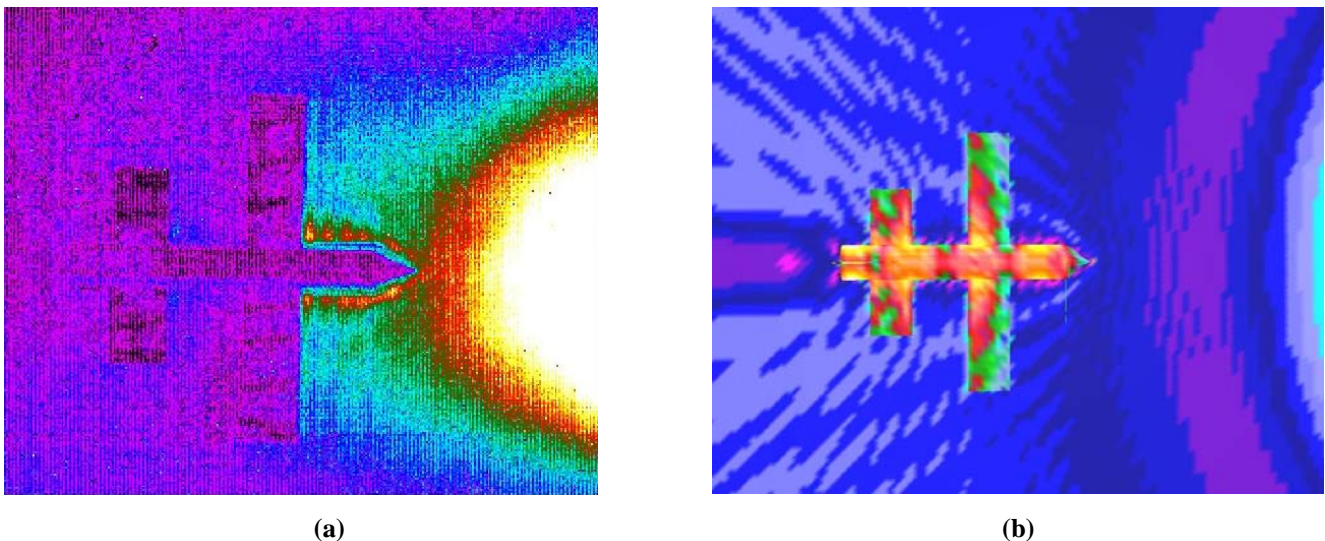
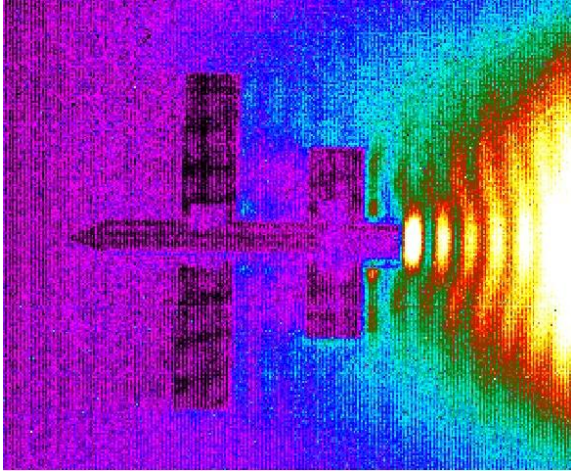
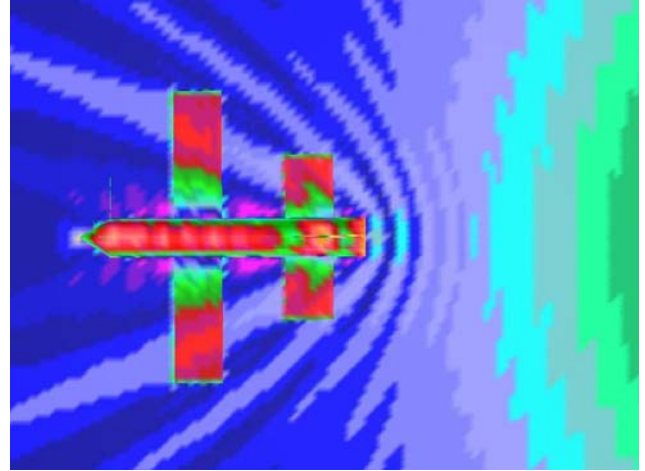


**Figure 4. Nose-On at 6GHz (Incident Spherical Wave)**  
**(a) Contour Map Showing Measured Relative Field Magnitudes Using the IR Technique, and**  
**(b) Contour Map Showing Relative Co-Pole Field Magnitudes Using the CEM Simulation Technique**



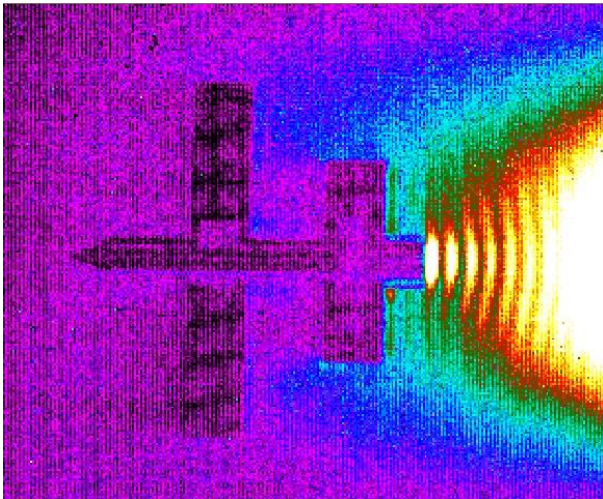
(a)



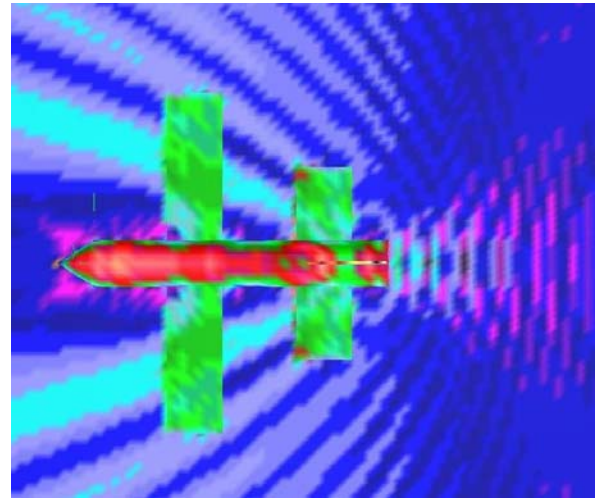
(b)

**Figure 5. Tail-On at 4GHz (Incident Spherical Wave)**

- (a) Contour Map Showing Measured Relative Field Magnitudes Using the IR Technique, and  
 (b) Contour Map Showing Relative Co-Pole Field Magnitudes Using the CEM Simulation Technique



(a)



(b)

**Figure 6. Tail-On at 6GHz (Incident Spherical Wave)**

- (a) Contour Map Showing Measured Relative Field Magnitudes Using the IR Technique, and  
 (b) Contour Map Showing Relative Co-Pole Field Magnitudes Using the CEM Simulation Technique

## 9.0 REFERENCES

- [1] J. D. Norgard and R. L. Musselman, "Direct IR Measurements of Phased Array Aperture Excitations," QIRT Journal, Vol. 2, No. 1, January 2005, pp.113-126.
- [2] J. D. Norgard and R. L. Musselman, "Direct IR Measurements of Phased Array Near-Field and Far-Field Antenna Patterns," QIRT Journal, Vol. 2, No. 2, July 2005, pp.223-236.
- [3] J. D. Norgard, R. Musselman, A. Drozd and I Kasperovich, "Validation and Verification of CEM Field Prediction Techniques Compared to IR Images of EM Fields for Complex Systems," 28<sup>th</sup> Annual AMTA Meeting & Symposium, Austin, TX, 24-26 October 2006, CD Conference Digest.



# Predicting and Mitigating Techniques of the PCB Rectangular Power/Ground Planes' Resonance Modes

Sungtek Kahng

Dept. of Information and Telecommunication Eng., University of Incheon, Incheon, Korea  
s-kahng@incheon.ac.kr

## ABSTRACT

The pair of metalized plates so called 'power/ground planes' or 'Power-Bus Structure' in the layered PCB architecture is known for causing the resonance phenomena that lead to increasing the impedance of the ground and finally becoming the noise in digital signal transfer in the PCB. In line with the signal integrity, it is necessary to predict the exact resonance behavior in the impedance as well as electromagnetic fields from the structure. For accurate evaluation of the electromagnetic properties due to the resonance, an efficient way of calculation 'series expansion' is used for the basic geometry and it is extended to the power-bus structure loaded with SMT(surface mounting technology) components for considering the resonance-mitigation by lumped elements. Besides, in an attempt to lower the impedance level of the ground, multiple feeds such as differential modes are adopted to provide the artificial return current path, and numerous cases of this particular feeding scheme are investigated with and without SMT loads. Finally, the radiated emission(RE) levels from the structure will be dealt with to see how the resonance mode ends up with the fields propagated from the edges of the power-bus geometry and what approaches can lower the RE level.

*Keywords* : PCB power/ground planes, Series Expansion, SMT component, RE, Resonance

## 1. INTRODUCTION

To facilitate the components and circuits for numerous essential functions in one body, modern communication systems are designed to have layers of PCBs. Standard layering of the PCBs has a pair of metal planes facing each other for DC-power supply and grounding. They are called power/ground planes.

The PCB power/ground planes form a cavity, composed of the top and bottom planes as the PEC boundary condition and the PMC walls[1-6]. These boundary value problems can be treated by a number of numerical techniques such as Method of Moment, Finite Difference Time Domain, Finite Element Method, etc. to examine physics on the structure generating resonance modes, impedance rise and interference problems. Among the computational techniques, a modal sum or series expansion analysis method is considered convenient to use when there is no problem in assuming the geometry as a cavity[1, 4-5].

Once we are convinced of the validity of the analysis method for the structure of this interest, we can move on to coping up with the resonance. In practice, SMT loads such as decoupling capacitors are placed on the plate on which PCB components reside. For the local elements to be included in the

process to remove the resonance and prediction, a number of times of linear algebraic manipulations are employed to carry out the Kirchhoff current and voltage laws. However, a simple expression is introduced later with the SMT application to reduce the impedance levels of resonance points. Furthermore, if multiple feeds are used to guarantee the return current path with respect to the original signal line, we will possibly improve the solution. This can be numerically characterized using the superposition principle without any difficulty and will show the differential multiple feeds can make things better

Along with the impedance watch and fields in the vicinity of the power-bus structure, it is important to check out the electromagnetic waves in the far zone from the cavity as Radiated Emission(RE) level, an indicator of electromagnetic interference toward adjacent circuits. This RE level can be predicted by the radiation integral, using the structure’s magnetic currents induced along the walls.

This paper is organized as follows. First, the modal analysis method to meet the boundary conditions of the power/ground planes results in the series expansion to calculate the fields and impedance of the unloaded power/ground planes and then it is modified to the geometry with lumped elements. Second, two feeding techniques with differential mode and common-mode are addressed and applied to reduce the impedance projections at resonance modes, with the aforementioned mathematical expression developed to the multiple cases by way of the superposition principle. Finally, we deal with the RE level which is a yardstick about the interference due to the resonance and discuss the lumped element loading and multiple feeding schemes for mitigating the RE levels.

**2. THEORY**

**2.1 Series Expansion Form for a Cavity Structure Analysis**

Lately, the PCB level EMC problems have drawn much attention for many reasons. One is that a variety of potential noise sources around the RF systems are formed by way of the layers in the PCB. The main noise maker is the power-bus structure which has resonance modes, illustrated as in Figure 1

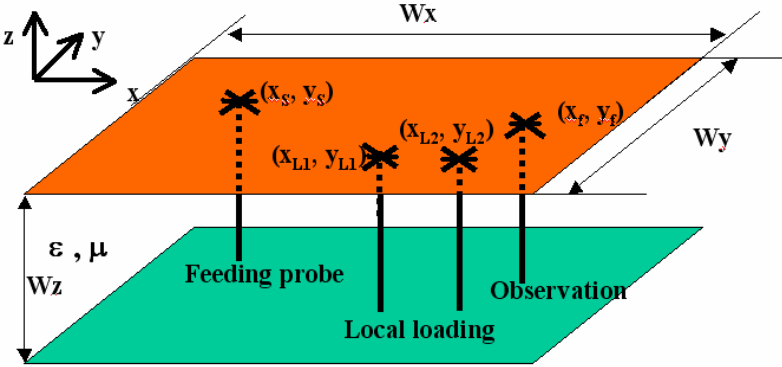


Fig. 1. Cavity model for a power/ground plane structure with ports and loads

The top as the ground and the bottom as the power-metal plane are identical in size with  $W_x \times W_y \times W_z$ . The DC current is carried along the feeding probe situated at  $(X_s, Y_s)$ . And it is used as port 1. Port 2 is any arbitrary observation point at  $(X_f, Y_f)$  where induced voltage is observed. The impedance from port  $s$  to port  $f$  is given as

$$Z_{s,f} = \sum_{m=0}^{\infty} \sum_{n=0}^{\infty} \frac{\gamma_{mn} \cdot c_{mn}(X_s, Y_s) \cdot c_{mn}(X_f, Y_f) \cdot W_z / (W_x W_y)}{\varepsilon\omega / Q + j(\varepsilon\omega - \frac{k_{xm}^2 + k_{yn}^2}{\omega\mu})} \quad (1)$$

The intermediate region between the two planes is the dielectric substrate and 4.2 and 0.02 are given as its relative dielectric constant and loss tangent, respectively. Referring to the structure's boundary conditions again, the two planes are the PEC and the walls are the PMC. Then, the impedance, when lumped elements are placed at  $(X_L, Y_L)$ , is expressed as[5]

$$Z_{Ld} = \sum_{m=0}^{\infty} \sum_{n=0}^{\infty} \frac{\gamma_{mn} \cdot c_{mn}(X_s, Y_s) \cdot c_{mn}(X_f, Y_f) \cdot W_z / (W_x W_y)}{\varepsilon\omega / Q + j(\varepsilon\omega - \frac{k_{xm}^2 + k_{yn}^2}{\omega\mu}) + \frac{\gamma_{mn} \cdot W_z}{W_x W_y} \sum_{Lu=1}^{NLu} c_{mn}^2(X_{Lu}, Y_{Lu}) \cdot \tilde{Y}_{Lu}} \quad (2)$$

where

$$c_{mn}(X_i, Y_i) = \cos(k_{xm} X_i) \cdot \cos(k_{yn} Y_i) \cdot \text{sinc}(k_{xm} P_{xi}/2) \cdot \text{sinc}(k_{yn} P_{yi}/2)$$

$$k_{xm} = m\pi / W_x, \quad k_{yn} = n\pi / W_y, \quad \omega = 2\pi f, \quad Q = [\tan \delta + \sqrt{2 / (\omega\mu_0 \kappa W_z^2)}]^{-1} \quad (3)$$

$\gamma_{mn}$  is 1 and 4 for  $(m=0, n=0)$  and  $(m \neq 0, n \neq 0)$  each. When  $(m \neq 0, n=0)$  or  $(m=0, n \neq 0)$ ,  $\gamma_{mn}$  takes 2.  $\tan \delta$ ,  $\varepsilon$ ,  $\mu$ ,  $f$ ,  $P_i$  and  $j$  denote loss-tangent, permittivity, permeability, frequency, port's width and  $\sqrt{-1}$ , respectively. Eqn. (1) considers  $N_{Lu}$  loads with the series equivalent circuit of the  $Lu$ -th load  $\tilde{Y}_{Lu} = [R_{Lu} + j(\omega L_{Lu} - 1/(\omega C_{Lu}))]^{-1}$  (4)

## 2.2 Structure with Multiple Feeds

By now, the things were about the one feed structure. Now let us talk about the multiple feeds.

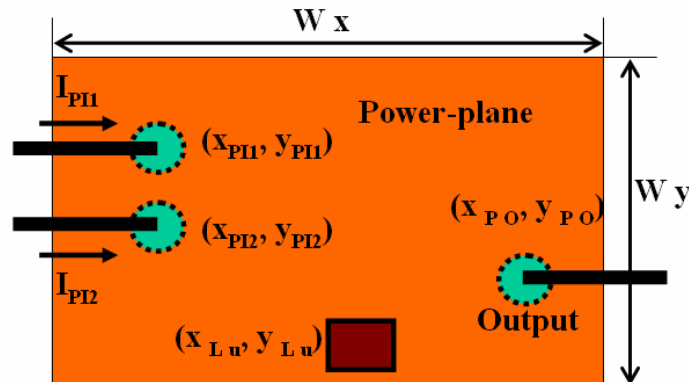


Fig. 2. Top-view of a power/ground plane structure with two feeds

Based upon the one-feeding line case, the differential signaling can be characterized with no difficulty, since the superposition principle also works in this structure. Therefore, the common-mode impedance and the differential-mode impedance are calculated by using the Eqn.'s (8) and (9) in [6].

### 2.3 Radiated Emission Characterization

Employing of the evaluation above, the electromagnetic field strength is shown to be maximum at resonance modes, and they propagate past the edges of the planes to the external region. This radiated emission(RE) from one cavity reaches its upper and lower PCB layers and nearby systems.

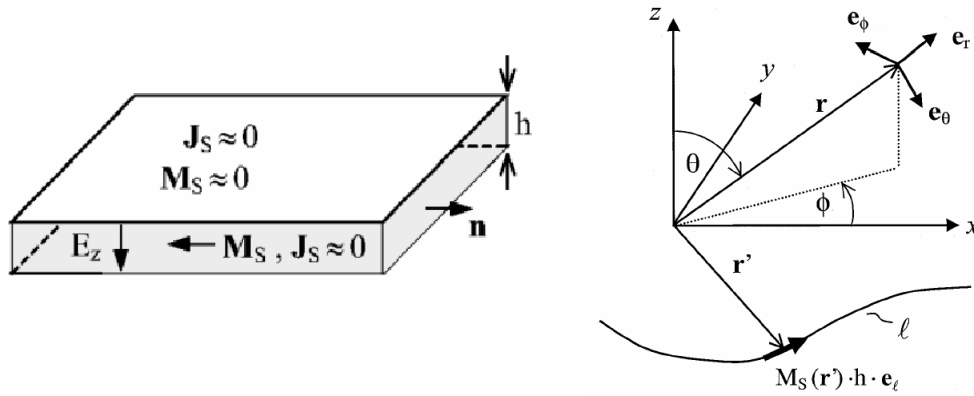


Fig. 3. Geometric configuration and coordinates of radiated emission[6]

The radiation can be explained as that of magnetic currents due to  $E_z$  is induced on the walls first, and then this fictitious current radiates. As for this, the radiation integral in the following is employed[6].

$$\underline{E} = (jk_0 W_z e^{jk_0 r} / (4\pi r)) \oint_{Rim} \underline{M}_s(r') e^{jk_0 r' \cdot \hat{e}_r} (\hat{e}_r \times \hat{e}_l) dl \quad (5)$$

$\underline{M}_s(r')$  is the induced magnetic current at  $\underline{r}'$  on the walls, and  $\hat{e}_r$  and  $\hat{e}_l$  are the normalized position vectors of the observation and source points.  $k_0$  is the free-space wave-number. Given that  $W_z$  is far less than  $W_x$  or  $W_y$  Eqn (5) takes a line integral along the periphery instead of a surface integral. Also, the above equation can be approximated as the far-zone field for simplicity.

### 3. RESULTS OF EXPERIMENTS

Firstly, the input impedance evaluation is performed using Eqn.(1) with respect to the power/ground planes of 220mm by 150mm by 1.5mm. And the DC current is fed at  $(X_s=0, Y_s=0)$  from bottom to top. The observation is made at the same as the source position, whose impedance is called 'self-impedance'. The frequency of interest for simulation ranges from 0 through 1GHz.

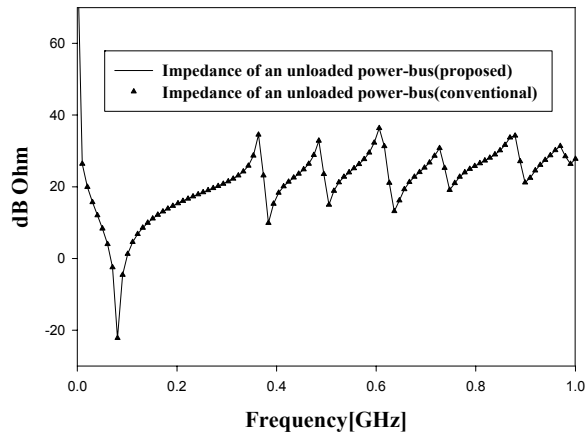


Fig. 3. Comparing the measurement and calculation for an unloaded structure's input impedance

The two methods produce the overlapping results. The series expansion was truncated at ( $m=400$ ,  $n=400$ ) and it can be made faster if a transformation (one-sided fourier transformation) is used. Seeing the result, beyond 200 MHz, peaks of resonance modes (1,0), (0,1), (1,1), (2,0), (2,1) and (0,2) occur in order.

Next, the power/ground plane structure is loaded with components. DeCaps are used in the structure. Resonance modes at 370MHz and 730MHz are targeted for damping by DeCaps. Using optimization techniques considering two DeCaps, the followings are obtained. DeCaps 1 and 2 have ( $1\Omega, 4.6nH, 47pF$ ) at (220mm, 75mm) and ( $12\Omega, 1.5nH, 47pF$ ) at (0, 75mm), respectively. In the second place, Eqn.(4) is used with those input parameters for  $Y_{NLoads}$  to present the damping performance on the desired resonance modes. In addition to the input impedance evaluation, the maximum of  $|\underline{E}|$  as RE level is calculated with respect to the original resonance modes. In particular, the RE levels of the power/ground planes before and after damping the specified resonance modes are compared along with the impedance profiles.

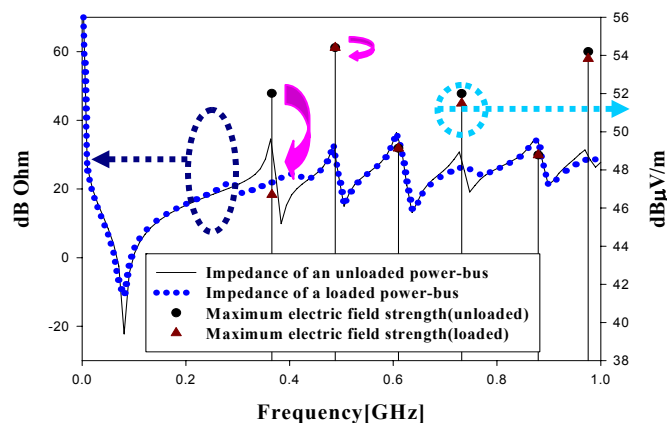


Fig. 4. Impedance and RE before and after loading DeCaps in the power/ground planes

Seeing the solid and dotted lines as the original power/ground planes and loaded case, the impedance levels at the aforementioned resonance modes are reduced by 13dB and 4dB as desired. This can be confirmed by the fact that the RE levels at 370MHz and 730MHz come down from 52 dB $\mu$ V/m and 52 dB $\mu$ V/m to 47 dB $\mu$ V/m and 51dB $\mu$ V/m, respectively. It is proven that the damping of the resonant impedance point can reduce the RE level out of the power/ground planes.

Now, the calculation of the impedance is carried out on the power-bus structure with the differential signals. Through this experiment, we will have an idea how accurate the proposed single-sum calculation is, when examined by the comparison with the results of the double-sum and the FDTD application for the same environment for simulation[7].

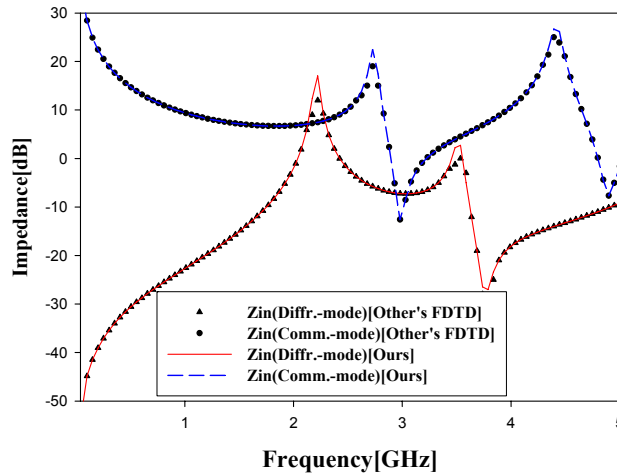


Fig. 5. Differential- & common-mode feeding results on the power/ground planes

The structure and frequency range are the same as [7], where 54mm $\times$ 33.5mm $\times$ 1.1mm, (27.0mm, 17.2mm), (27.0mm, 16.3mm), (41.8mm, 27.4mm) are given to  $W_x \times W_y \times W_z$ ,  $(X_{P0}, Y_{P0})$ ,  $(X_{N0}, Y_{N0})$ , and  $(X, Y)$ . Fig. 5 shows the good agreement between the present method and the FDTD in [7] except for negligible discrepancies at some peaks. Seeing the compared curves of the two feed signals, the differential mode has lower impedance than the common-mode, and is superior to the one-feed case when good conditions are met such as right placement and proper distance between the feeds in practice The following is the RE prediction with the differential feeding as well as common-mode feeding

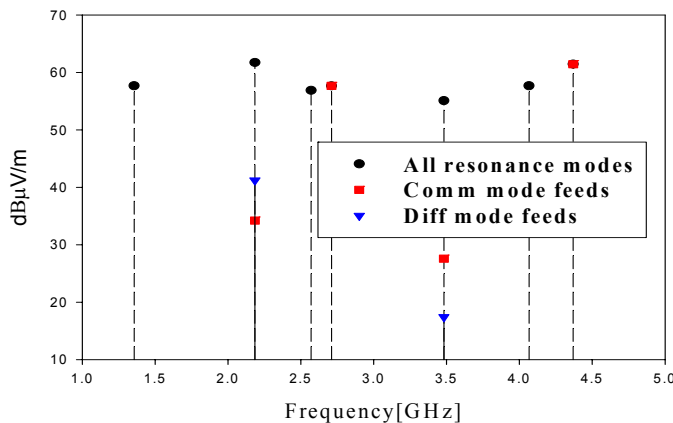
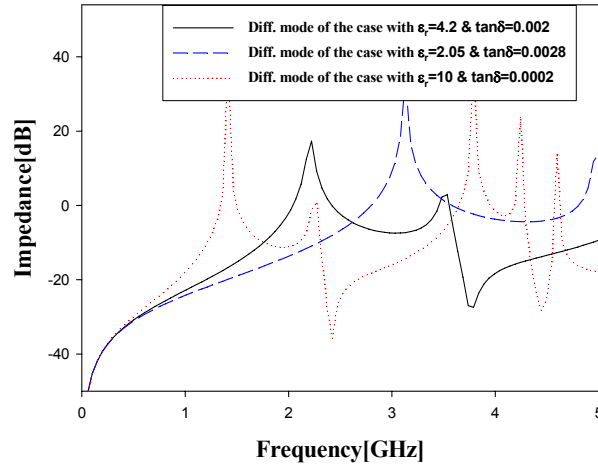


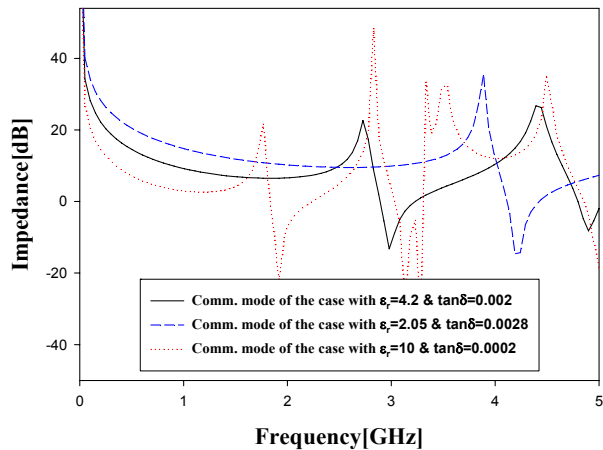
Fig. 6. Differential- & common-mode feeding V.S. RE levels

Examining the comparison, the improvement is found at the resonance frequencies of the original one feed structure to the reduced RE level introduced by the two feed system..

Finally, we will observe the trend of the impedance profile according to the different conditions on the multiple feeding. Different kinds of substrate materials will be input.



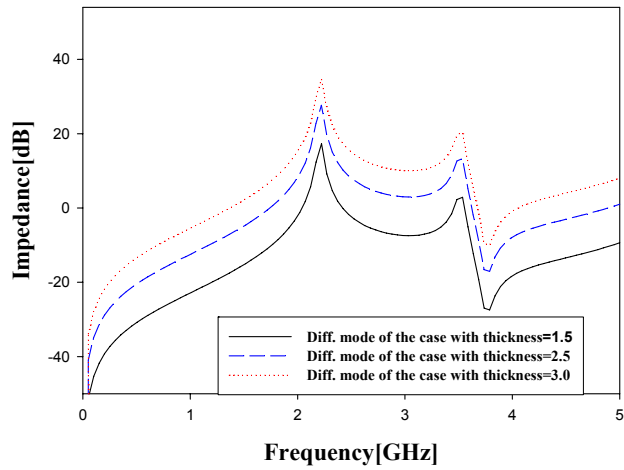
(a) Differential mode signals



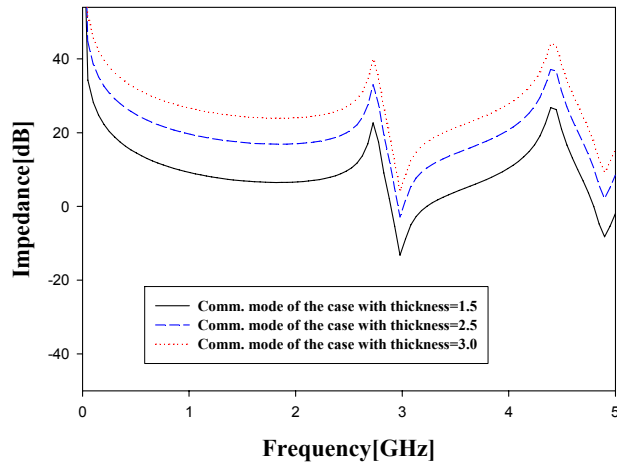
(b) Common-mode signals

Fig. 7. Effects of the different dielectric constants and loss tangent values

The solid lines in Fig.'s 6 (a) and (b) correspond to the differential and common mode signals in Fig. 8 used as the reference toward the change. As is seen, the change in the dielectric constant gives rise to a noticeable frequency shift. Regarding the differential mode signaling, the main peak (2 GHz) of the impedance moves from 3 GHz through 2GHz to 1 GHz, as the magnitude of the complex relative permittivity increases. On the contrary to the former(out-of-phase) signaling, the common-mode(in-phase) signaling does not show a fixed pattern. What comes next is the influence of the change in the thickness of the spacing between the power- and ground planes.



(a) Differential mode signals



(b) Common mode signals

Fig. 8. Effects of the different spacing between the power/ground planes

In Fig. 8, the thicker substrate causes the impedance profiles to increase in both common mode as well as differential mode. As is addressed before, the varied spacing between the two plates fixes the resonance modes with lowered capacitance and increased inductance of the structure, but extends current paths on the metal planes.

#### 4. CONCLUSION

PCB power/ground planes have been rigorously characterized by the modal summation expansion. In particular, the resonance modes have been predicted with the impedance and fields in the structure. Given a valid method of calculation, the formula could be extended to the loaded structure and differential mode and common-mode feeding in an effort to decrease the impedance peaks at the resonance modes. Besides, the interference due to the radiated emission has been investigated by



another simple computational method and validated by measurement. These things are very important to get the idea on how to cope with the damping of the resonance and leave the door open to find the best answer for a determined geometry for practical work.

## REFERENCES

- [1] T. Okoshi, *Planar Circuits for Microwaves and Lightwaves*, Berlin, Germany: Springer-Verlag, 1985.
- [2] S. Kahng, "Study on reducing common-mode current on a wire through an aperture with a ring stack," in *Proc. EMC Zurich, Switzerland, 2005*, pp.585-58.
- [3] M. Xu, H. Wang, and T. H. Hubing, "Application of the cavity model to lossy power-return plane structures in printed circuit boards," *IEEE Trans. Adv. Packag.*, Vol. 26, pp.73-80, Feb. 2003.
- [4] Z. L. Wang, O. Wada, Y. Toyota, and R. Koga, "Convergence Acceleration and Accuracy Improvement in Power Bus Impedance Calculation with a Fast Algorithm using Cavity Modes," *IEEE Trans. Electromagn. Compat.*, vol. 47, pp. 2-9, February 2005.
- [5] M. Hampe, and S. Dickmann, "The impact of decoupling capacitors on the impedance of rectangular PCB power-bus structures," in *Proc. EMC Zurich, Switzerland, 2005*, pp.251-256.
- [6] M. Leone, "The radiation of a rectangular power-bus structure at multiple cavity-mode resonances," *IEEE Trans. Electromagn. Compat.*, Vol. 40, pp.113-118, Feb. 2003

**PERMANENT STANDING COMMITTEES OF ACES, INC.**

<b>COMMITTEE</b>	<b>CHAIRMAN</b>	<b>ADDRESS</b>
NOMINATION	Randy Haupt	Penn State University PO Box 30 State College, PA 16804-0030 <a href="mailto:rlh45@psu.edu">rlh45@psu.edu</a>
ELECTIONS	Amir Zaghloul	Bradley ECE Dept. Virginia Polytech. Inst. & State U. 7054 Haycock Rd., Rm. 416 Falls Church, VA 22043 <a href="mailto:amirz@vt.edu">amirz@vt.edu</a>
AWARDS	Randy Haupt	Penn State University PO Box 30 State College, PA 16804-0030 <a href="mailto:rlh45@psu.edu">rlh45@psu.edu</a>
FINANCE	Andrew Peterson	Georgia Institute of Technology School of ECE Atlanta, GA 30332-0250 <a href="mailto:peterson@ece.gatech.edu">peterson@ece.gatech.edu</a>
PUBLICATIONS	Atef Elsherbeni	EE Department, Anderson Hall University of Mississippi University, MS 38677 <a href="mailto:atef@olemiss.edu">atef@olemiss.edu</a>
CONFERENCE	Osama Mohammed	Florida International University ECE Department Miami, FL 33174 <a href="mailto:mohammed@fiu.edu">mohammed@fiu.edu</a>

<b>MEMBERSHIP ACTIVITY COMMITTEES OF ACES, INC.</b>
---

<b>COMMITTEE</b>	<b>CHAIRMAN</b>	<b>ADDRESS</b>
SOFTWARE VALIDATION	Bruce Archambeault	IBM 3039 Cornwallis Road, PO Box 12195 Dept. 18DA B306 Research Triangle Park NC 27709
HISTORICAL	(Vacant)	
CONSTITUTION & BYLAWS	Natalia K. Nikolova	Dept of Electrical & Computer Engineering, ITB/A220 McMaster University 1280 Main Street West, Hamilton, ON L8S 4K1, Canada <a href="mailto:talia@mcmaster.ca">talia@mcmaster.ca</a>
MEMBERSHIP & COMMUNICATIONS	Vicente Rodriguez	ETS-LINDGREN L.P. 1301 Arrow Point Drive Cedar Park, TX 78613 <a href="mailto:rodriguez@ieee.org">rodriguez@ieee.org</a>
INDUSTRIAL RELATIONS	Andy Drozd	ANDRO Consulting Services PO Box 543 Rome, NY 13442-0543 <a href="mailto:andro1@aol.com">andro1@aol.com</a>
MEMBERSHIP GRADES	Randy Haupt	<a href="mailto:rlh45@psu.edu">rlh45@psu.edu</a>

## ACES NEWSLETTER STAFF

### EDITOR-IN-CHIEF, NEWSLETTER

Alistair Duffy  
De Montfort University  
The Gateway  
Leicester  
LE1 9BH United Kingdom  
Phone: +44 (116) 257 7056  
email: [apd@dmu.ac.uk](mailto:apd@dmu.ac.uk)

### EDITOR-IN-CHIEF, PUBLICATIONS

Atef Elsherbeni  
Electrical Engineering Department,  
Anderson Hall, Box 13  
University of Mississippi  
University, MS 38677  
Phone: 662-915-5382  
email: [atef@olemiss.edu](mailto:atef@olemiss.edu)

### ASSOCIATE EDITOR-IN-CHIEF

Ray Perez  
Martin Marietta Astronautics  
MS 58700, PO Box 179  
Denver, CO 80201  
Phone: 303-977-5845  
Fax: 303-971-4306  
email: [ray.j.perez@lmco.com](mailto:ray.j.perez@lmco.com)

### MANAGING EDITOR

Richard W. Adler  
Naval Postgraduate School/ECE Dept.  
Code ECAB, 833 Dyer Road,  
Monterey, CA 93943-5121  
Fax: 831-649-0300  
Phone: 831-646-1111  
email: [rwa@att.biz](mailto:rwa@att.biz)

## EDITORS

### CEM NEWS FROM EUROPE

Tony Brown  
University of Manchester  
PO Box 88 Sackville Street  
Manchester M60 1QD United Kingdom  
Phone: +44 (0) 161-200-4779  
Fax: +44 (0) 161-200-8712  
email: [Anthony.brown@manchester.ac.uk](mailto:Anthony.brown@manchester.ac.uk)

### TECHNICAL FEATURE ARTICLE

Andy Drodz  
ANDRO Consulting Services  
PO Box 543  
Rome, NY 13442-0543  
Phone: 315-337-4396  
Fax: 314-337-4396  
email: [androl@aol.com](mailto:androl@aol.com)

### THE PRACTICAL CEMIST

W. Perry Wheless, Jr.  
University of Alabama  
PO Box 11134  
Tuscaloosa, AL 35486-3008  
Phone: 205-348-1757  
Fax: 205-348-6959  
email: [wwheless@coe.eng.ua.edu](mailto:wwheless@coe.eng.ua.edu)

### MODELER'S NOTES

Gerald Burke  
Lawrence Livermore National Labs.  
Box 5504/L-156  
Livermore, CA 94550  
Phone: 510-422-8414  
Fax: 510-422-3013  
email: [burke2@llnl.gov](mailto:burke2@llnl.gov)

### PERSPECTIVES IN CEM

Alistair Duffy  
School of Engineering and Technology  
De Montfort University  
The Gateway  
Leicester, UK LE1 9BH  
+44(0)116 257 7056  
email: [apd@dmn.ac.uk](mailto:apd@dmn.ac.uk)

### TUTORIAL

Giulio Antonini  
UAq EMC Laboratory  
Department of Electrical Engineering  
University of L'Aquila  
Poggio di Roio, 67040 Italy  
Phone: +39-0862-43446  
email: [antonini@ing.univaq.it](mailto:antonini@ing.univaq.it)

## ACES JOURNAL

### EDITOR-IN-CHIEF

Atef Elsherbeni  
University of Mississippi  
Electrical Engineering Dept.  
Anderson Hall, Box 13  
University MS 38677  
Phone: 662-915-5382  
email: [atef@olemiss.edu](mailto:atef@olemiss.edu)

### ASSOCIATE EDITOR-IN-CHIEF

Erdem Topksakal  
Mississippi State University  
ECE Department  
405 Simrall Hall, Hardy St.  
Mississippi State, MS 39762  
Phone: 662-325-2298  
email: [toksakal@ece.msstate.edu](mailto:toksakal@ece.msstate.edu)

## NEWSLETTER ARTICLES AND VOLUNTEERS WELCOME

The ACES Newsletter is always looking for articles, letters and short communications of interest to ACES members. All individuals are encouraged to write, suggest or solicit articles either on a one-time or continuing basis. Please contact a Newsletter Editor.

## AUTHORSHIP AND BERNE COPYRIGHT CONVENTION

The opinions, statements and facts contained in this Newsletter are solely the opinions of the authors and/or sources identified with each article. Articles with no author can be attributed to the editors or to the committee head in the case of committee reports. The United States recently became part of the Berne Copyright Convention. Under the Berne Convention, the copyright for an article in this newsletter is legally held by the author(s) of the article since no explicit copyright notice appears in the newsletter.

### BOARD OF DIRECTORS

#### EXECUTIVE COMMITTEE

Osama Mohammed, President  
Atef Elsherbeni, Vice President  
Natalia Nikolova, Secretary

Allen W. Glisson, Treasurer  
Richard W. Adler, Executive Officer

#### DIRECTORS-AT-LARGE

Atef Elsherbeni	2008	C.J. Reddy	2009	Allen Glisson	2010
Michiko Kuroda	2008	Osama Mohamed	2009	Samari Baramada	2010
Andrew Drozd	2008	Natalia Nikolova	2009	Amir Zaghloul	2010

### ACES ELECTRONIC PUBLISHING GROUP

Atef Elsherbeni	Electronic Publishing Managing Editor
Matthew J. Inman	Site Administrator
Mohamed Al Sharkawy	Contributing Staff
Imran Kader	Past Site Administrator
Orin H. Council	Past Staff
Brad Baker	Past Staff
Jessica Drewrey	Past Staff
Chris Riley	Past Staff

Visit us on line at:  
<http://aces.ee.olemiss.edu>

<b>ADVERTISING RATES</b>		
	<b>FEE</b>	<b>PRINTED SIZE</b>
Full page	\$200	7.5" × 10.0"
1/2 page	\$100	7.5" × 4.7" or 3.5" × 10.0"
1/4 page	\$50	3.5" × 4.7"
<p>All ads must be camera-ready copy.</p> <p>Ad deadlines are same as Newsletter copy deadlines.</p> <p>Place ads with Alistair Duffy <a href="mailto:apd@dmu.ac.uk">apd@dmu.ac.uk</a>.</p> <p>The editor reserves the right to reject ads.</p>		

<b>DEADLINE FOR THE SUBMISSION OF ARTICLES</b>	
<b>Issue</b>	<b>Copy Deadline</b>
March	January 1
July	May 1
November	September 1

For the **ACES NEWSLETTER**, send copy to Alistair Duffy ([apd@dmu.ac.uk](mailto:apd@dmu.ac.uk)) in the following formats:

1. A PDF copy.
2. A MS Word (ver. 97 or higher) copy. If any software other than WORD has been used, contact the Managing Editor, Richard W. Adler **before** submitting a diskette, CD-R or electronic file.

<b>LAST WORD</b>
------------------

“Magnetism is one of the Six Fundamental Forces of the Universe, with the other five being Gravity, Duct Tape, Whining, Remote Control, and the Force that Pulls Dogs toward the Groins of Strangers.”

Dave Barry – writer and humorist